Electronic and Optical Properties of Orthorhombic $(CH_3NH_3)BX_3$ (B=Sn, Pb; X=F, Cl, Br, I) Perovskites: a First-Principles Investigation

Sean Nations[1,2], Ting Jia[1], Shengnian Wang[2], Yuhua Duan[1*]

[1] *National Energy Technology Laboratory, United States Department of Energy, Pittsburgh, Pennsylvania 15236, USA*

[2] *Chemical Engineering Department, Louisiana Tech University, Ruston, Louisiana 71272, USA*

Supplementary Materials

Contents

* Author to whom correspondence should be addressed. Tel. 412-386-5771, Fax 412-386-5990, E-mail: yuhua.duan@netl.doe.gov

A Fractional Coordinates

Table S1: Fractional coordinates for $(CH_3NH_3)SnF_3$ with *Pnma* symmetry.

Elements	Fractional Coordinates (Å)		
	x	*y*	*z*
H	0.064	0.388	0.847
H	0.963	0.343	0.159
H	0.837	0.250	0.882
H	0.204	0.250	0.127
C	0.034	0.250	0.102
N	0.996	0.250	0.906
F	0.278	0.971	0.274
F	0.044	0.250	0.513
Sn	1.000	0.000	0.500

Table S2: Fractional coordinates for $(CH_3NH_3)SnCl_3$ with *Pnma* symmetry.

Elements	Fractional Coordinates (Å)		
	x	*y*	*z*
H	0.524	0.324	0.851
H	0.481	0.329	0.137
H	0.339	0.250	0.902
H	0.678	0.250	0.083
C	0.533	0.250	0.079
N	0.476	0.250	0.910
Cl	0.787	0.975	0.281
Cl	0.540	0.250	0.496
Sn	0.500	0.000	0.500

Table S3: Fractional coordinates for $(CH_3NH_3)SnBr_3$ with *Pnma* symmetry.

Elements	Fractional Coordinates (Å)		
	x	*y*	*z*
H	0.010	0.321	0.851
H	0.984	0.326	0.127
H	0.837	0.250	0.907
H	0.169	0.250	0.067
C	0.031	0.250	0.070
N	0.967	0.250	0.909
Br	0.291	0.976	0.284

Br	0.037	0.250	0.490
Sn	1.000	0.000	0.500

Table S4: Fractional coordinates for $(CH_3NH_3)SnI_3$ with *Pnma* symmetry.

Elements	Fractional Coordinates (Å)		
	x	*y*	*z*
H	0.998	0.316	0.855
H	0.989	0.321	0.119
H	0.839	0.250	0.916
H	0.158	0.250	0.053
C	0.029	0.250	0.062
N	0.961	0.250	0.912
I	0.298	0.978	0.292
I	0.034	0.250	0.485
Sn	1.000	0.000	0.500

Table S5: Fractional coordinates for $(CH_3NH_3)PbF_3$ with *Pnma* symmetry.

Elements	Fractional Coordinates (˚A)		
	x	*y*	*z*
H	0.058	0.336	0.847
H	0.971	0.341	0.158
H	0.832	0.250	0.890
H	0.209	0.250	0.118
C	0.040	0.250	0.099
N	0.993	0.250	0.907
F	0.290	0.970	0.280
F	0.052	0.250	0.512
Pb	1.000	0.000	0.500

Table S6: Fractional coordinates for $(CH_3NH_3)PbBr_3$ with *Pnma* symmetry.

Elements	Fractional Coordinates (Å) *x*		
		y	*z*
H	0.509	0.320	0.854
H	0.484	0.324	0.127
H	0.336	0.250	0.911
H	0.667	0.250	0.067
C	0.530	0.250	0.070
N	0.466	0.250	0.912

Br	0.801	0.973	0.292
Br	0.542	0.250	0.489
Pb	0.500	0.000	0.500

Table S7: Fractional coordinates for $(CH_3NH_3)PbI_3$ with *Pnma* symmetry.

Elements	Fractional Coordinates (Å)		
	x	*y*	*z*
H	0.998	0.315	0.858
H	0.991	0.320	0.119
H	0.840	0.250	0.920
H	0.158	0.250	0.053
C	0.030	0.250	0.062
N	0.961	0.250	0.915
I	0.310	0.975	0.301
I	0.040	0.250	0.485
Pb	1.000	0.000	0.500

Table S8: The optimized atomic coordinates and energies of AX and BX_2 (B=Sn, Pb; X= F, Cl, Br, I),.

Material	Spacegroup	Lattice Constant (Å)			Volume ($Å^3$)	Energy $(\frac{eV}{formulation})$
		A	*B*	*C*		
(MA)F	Pbcm	4.5839	4.6717	6.9091	145.4501	-45.03644
(MA)Cl	Pbcm	5.4988	5.3658	7.7566	227.3162	-43.53056
(MA)Br	Pbcm	5.7145	5.5862	8.0935	256.785	-42.96261
(MA)I	Pbcm	6.0111	5.9031	8.5252	301.5837	-42.33157
SnF_2	Pnma	4.5356	4.9523	11.0505	248.2138	-14.22044
$SnCl_2$	Pnma	5.6740	5.8095	13.3720	440.7834	-10.51250
$SnBr_2$	Pnma	5.9604	5.9668	13.2283	470.4643	-9.44487
SnI_2	Pnma	6.3696	6.3693	13.4606	546.0927	-8.36619
PbF_2	Pnma	4.7428	4.6413	12.0883	266.0966	-14.18718
$PbCl_2$	Pnma	5.7308	5.7328	13.8380	454.6211	-10.68565
$PbBr_2$	Pnma	6.0520	6.0544	13.9399	510.7766	-9.60245
PbI_2	Pnma	6.4909	6.4943	13.9981	590.0778	-8.46915

B Bulk-Modulus

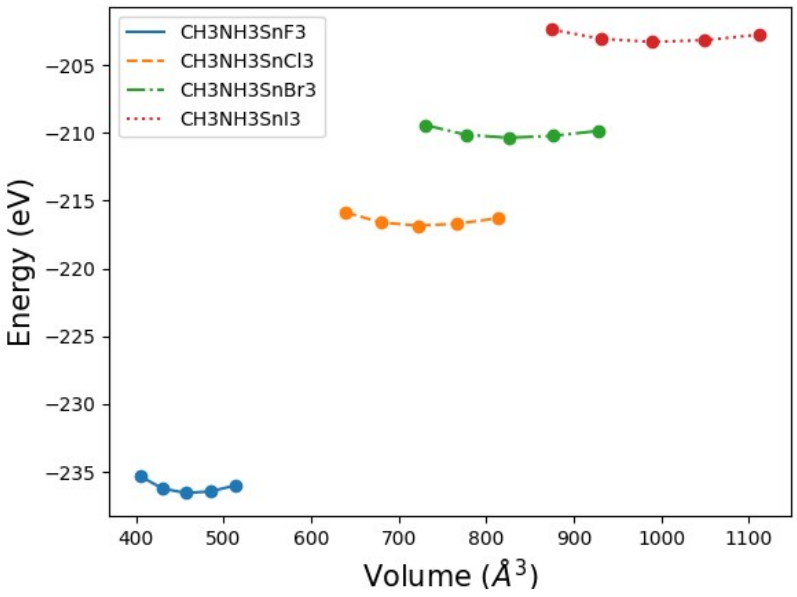

Figure S1: Energy versus volume for $(CH_3NH_3)SnX_3$ (X=F, Cl, Br, I) perovskites.

C Band-structure and Density of States

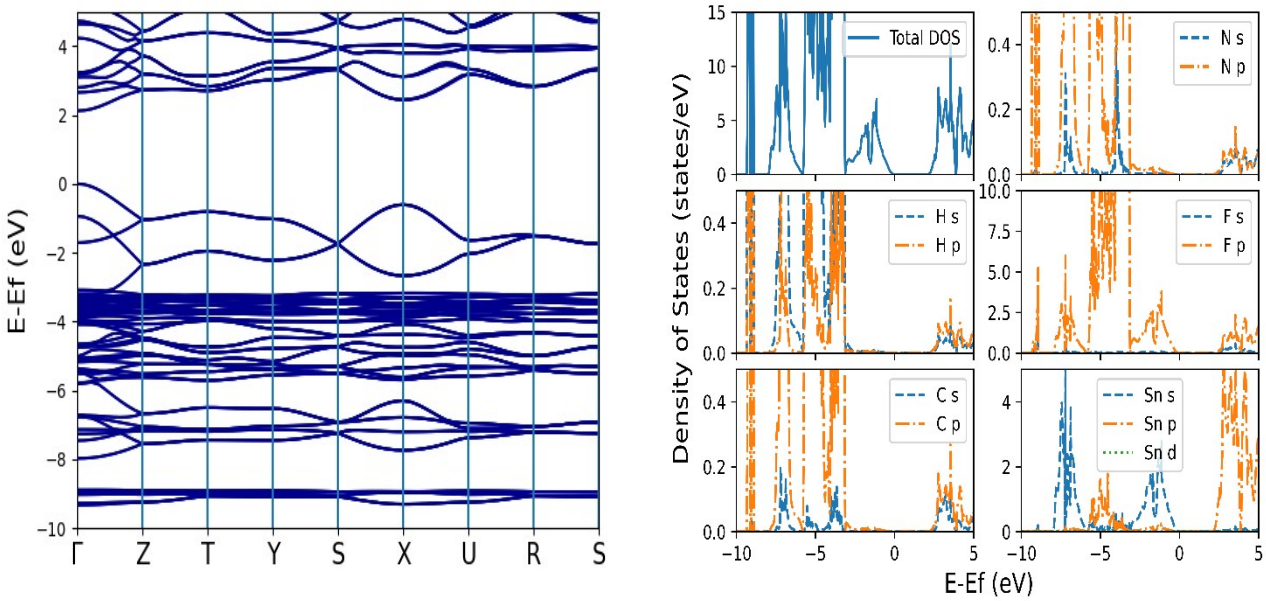

(a) (b)

Fig. S2: The calculated electronic structural properties for $(MA)SnF_3$: (a) band structure; (b) total and partial density of states.

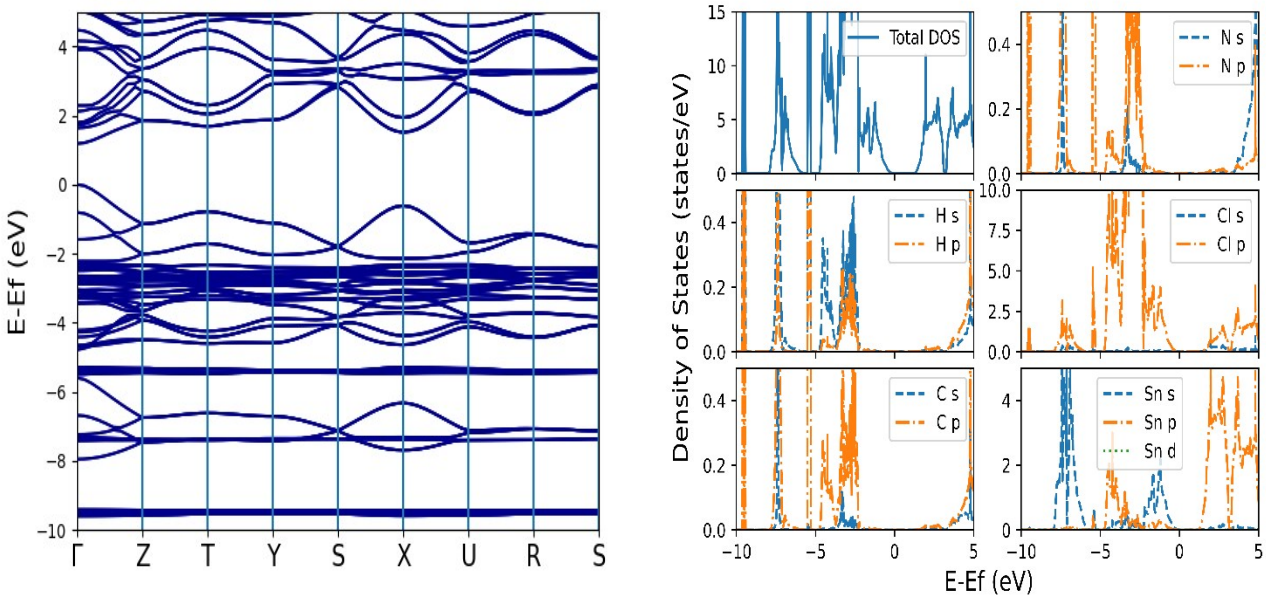

(a) (b)

Fig. S3: The calculated electronic structural properties for (MA)$SnCl_3$: (a) band structure; (b) total and partial density of states.

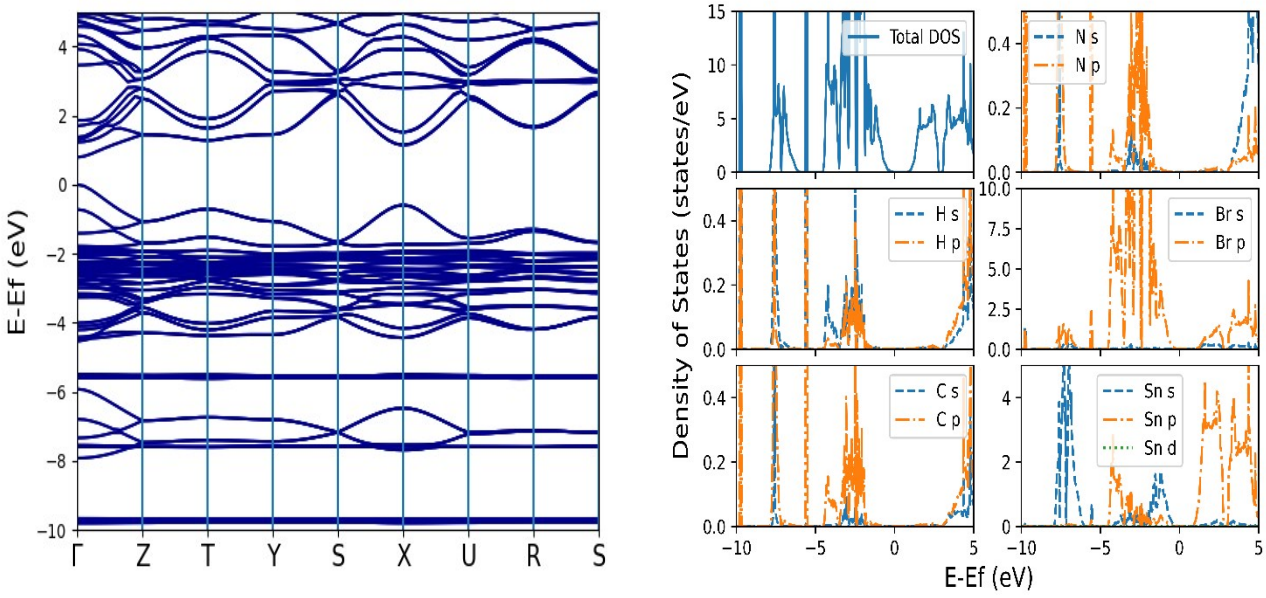

(a) (b)

Fig. S4: The calculated electronic structural properties for (MA)$SnBr_3$: (a) band structure; (b) total and partial density of states.

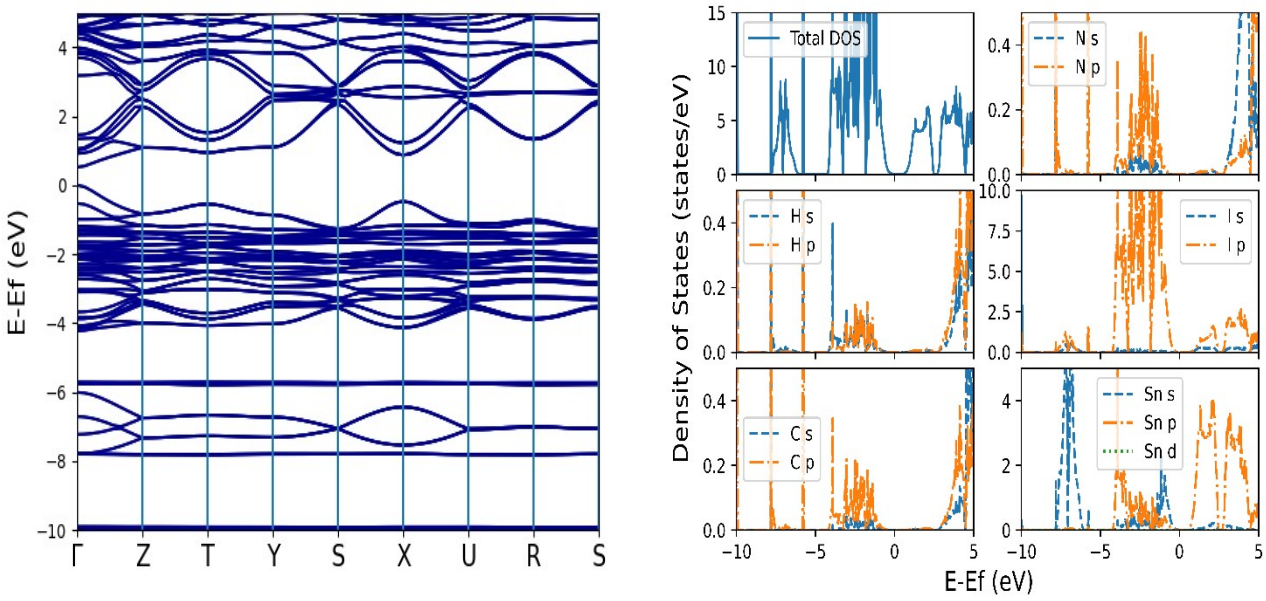

(a) (b)

Fig. S5: The calculated electronic structural properties for (MA)SnI_3: (a) band structure; (b) total and partial density of states.

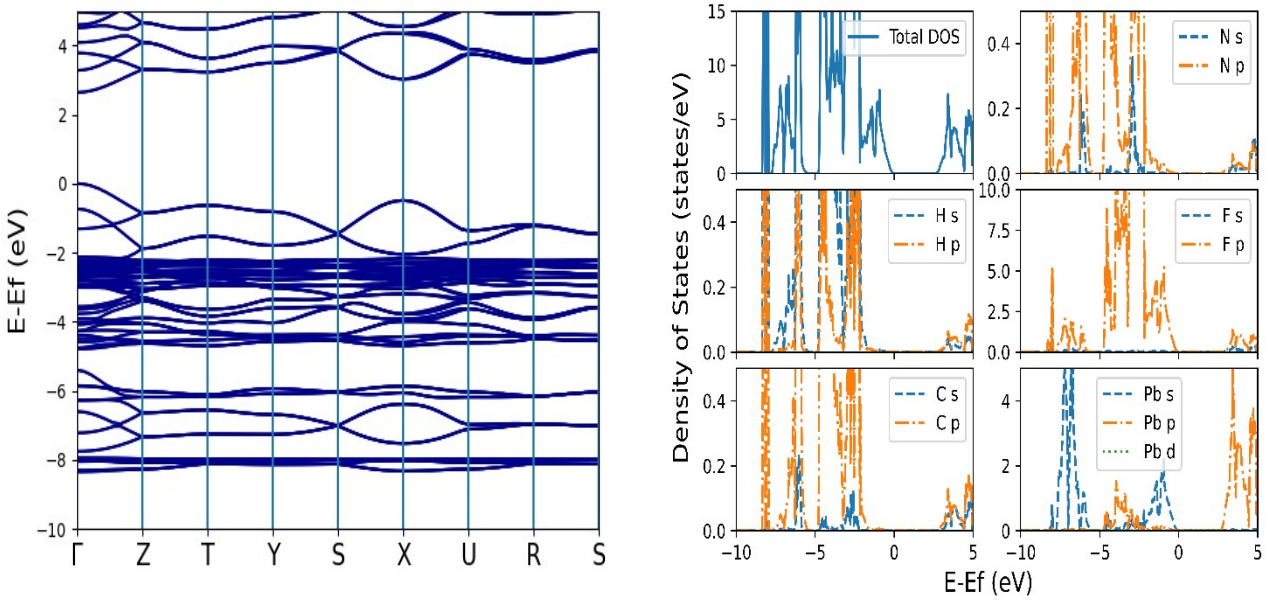

(a) (b)

Fig. S6: The calculated electronic structural properties for (MA)PbF_3: (a) band structure; (b) total and partial density of states.

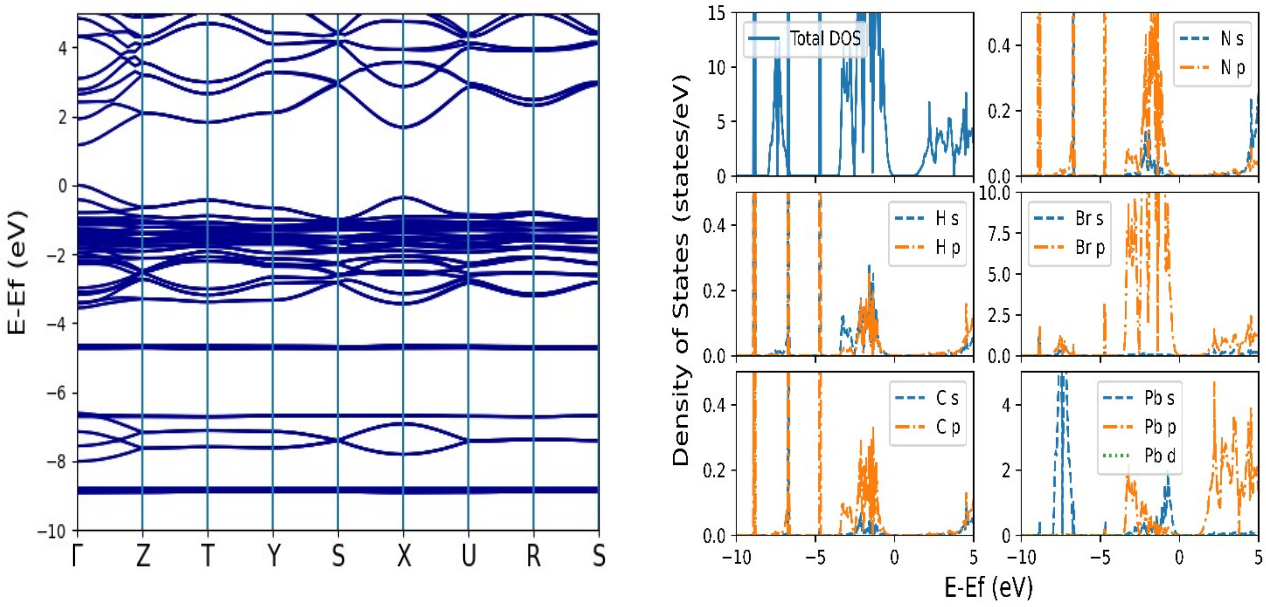

(a) (b)

Fig. S7: The calculated electronic structural properties for (MA)$PbBr_3$: (a) band structure; (b) total and partial density of states.

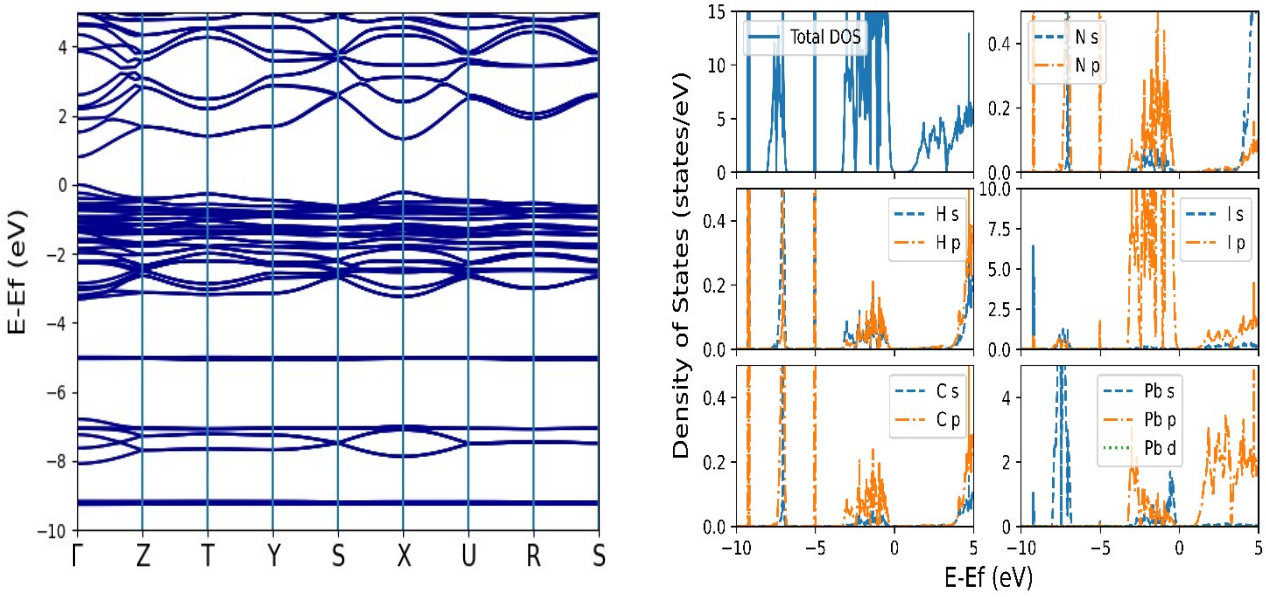

(a) (b)

Fig. S8: The calculated electronic structural properties for (MA)PbI_3: (a) band structure; (b) total and partial density of states.

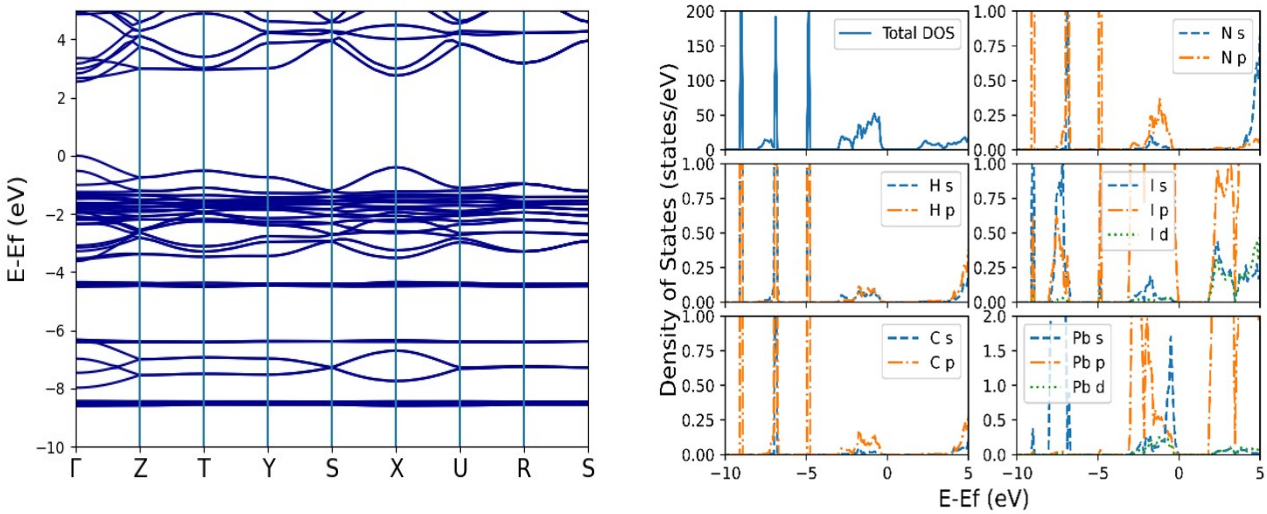

(a) (b)

Fig. S9: The calculated electronic structural properties for (MA)$PbCl_3$: (a) band structure; (b) total and partial density of states. Here, non-SOC calculations are presented for comparison with Figure 3 from the main document.

D Optics

D.1 Theory

To study the optical properties, the frequency-dependent dielectric matrix in the long wavelength limit (q→0) can be calculated using the sum over states approach.[1] The formula for the imaginary part of the dielectric constant is a 3x3 Cartesian tensor

$$\varepsilon_2^{\alpha\beta}(\omega) = \frac{4\pi^2 e^2}{\Omega}\lim_{q\to 0}\frac{1}{q^2}\sum_{c,v,k} 2\omega_k \delta(\epsilon_{ck} - \epsilon_{vk} - \omega) \times < u_{ck+e_\alpha q} | u_{vk} >< u_{ck+e_\beta q} | u_{vk} >^* \quad (1)$$

where the indices *c* and υ correspond to the conduction and valence band states, respectively and $u_{c\kappa}$ is the periodic part of the orbitals at the k-point κ. The vector $\mathbf{e}_\alpha$ are unit vectors for the three Cartesian directions. α and β refer to axis *x*, *y*, *z*. The real part of the dielectric constant tensor can be derived from the imaginary part using Kramers-Kronig relations:

$$\varepsilon_1^{\alpha\beta}(\omega) = 1 + \frac{2}{\pi} P \int_0^\infty \frac{\varepsilon_2^{\alpha\beta}(\omega')\omega'}{\omega'^2 - \omega^2} d\omega' \quad (2)$$

where P denotes the principal value. The real part of the optical conductivity (σ(ω)) is defined as

$$\sigma_1(\omega) = Re[\sigma(\omega)] = \frac{\omega}{4\pi}\varepsilon_2(\omega) \quad (3)$$

where σ(ω) and ω are in the cgs unit of sec^{-1}. The cgs conductivity is 9×10^{11} times larger than the SI conductivity unit (Siemens/cm) which in the form of $\sigma_1(\omega) = \frac{\varepsilon_2(\omega)\cdot\omega}{60}$ where ω is in the unit of cm^{-1}. The corresponding imaginary part of σ(ω) in SI unit is [2]

$$\sigma_2(\omega) = -\frac{\omega(\varepsilon_1(\omega) - 1)}{60} \tag{4}$$

The complex dielectric constant can be expressed as:

$$\varepsilon(\omega) = \varepsilon_1(\omega) + i\varepsilon_2(\omega) = \frac{4\pi i}{\omega}\sigma(\omega) = (\tilde{n} + i\tilde{k})^2 \tag{5}$$

where $\tilde{n}\ and\ \tilde{k}$ are the index of refraction and the extinction coefficient respectively, and can be evaluated by the calculated dielectric constants from equations (1) and (2).

$$\tilde{n} = \frac{1}{\sqrt{2}}(\varepsilon_1 + (\varepsilon_1^2 + \varepsilon_2^2)^{\frac{1}{2}})^{\frac{1}{2}} \tag{6}$$

$$\tilde{\kappa} = \frac{1}{\sqrt{2}}(-\varepsilon_1 + (\varepsilon_1^2 + \varepsilon_2^2)^{\frac{1}{2}})^{\frac{1}{2}} \tag{7}$$

In the case of normal incidence, the reflectivity R and the absorption coefficient α (sec^{-1} in cgs unit) in terms of $\tilde{n}\ and\ \tilde{k}$ are defined as [2]

$$R = \frac{(\tilde{n} - 1)^2 + \tilde{k}}{(\tilde{n} + 1)^2 + \tilde{k}} \tag{8}$$

$$\alpha = \frac{2\omega\tilde{k}}{c} \tag{9}$$

In SI unit, ω and α are in cm^{-1}, $\alpha=4\pi\omega\tilde{k}$. In all cases, both the low frequency region $\omega\tau \ll 1$ (τ is the relaxation time) and the high frequency region $\omega\tau \gg 1$ are extensively studied to analyze the exact ground state of the material as these two regions carry the signatures of two distinct mechanisms associated with optical conductivity within a solid. While the low frequency region is dominated by free carriers which are in abundance in a metal, the high frequency region is dominated by inter-band electronic transitions typical of a dielectric material. As in the limit $\omega\tau \ll 1$, both $\tilde{n}\ and\ \tilde{k}$ become sufficiently large, for example, in a metallic conductor,

$$R = 1 - \frac{2}{\tilde{n}} \to 1 \tag{10}$$

which means that the conductor is characterized by its behavior as a perfect reflector with an exceedingly large absorption coefficient in the low frequency region.

D.2 Halogen Comparisons

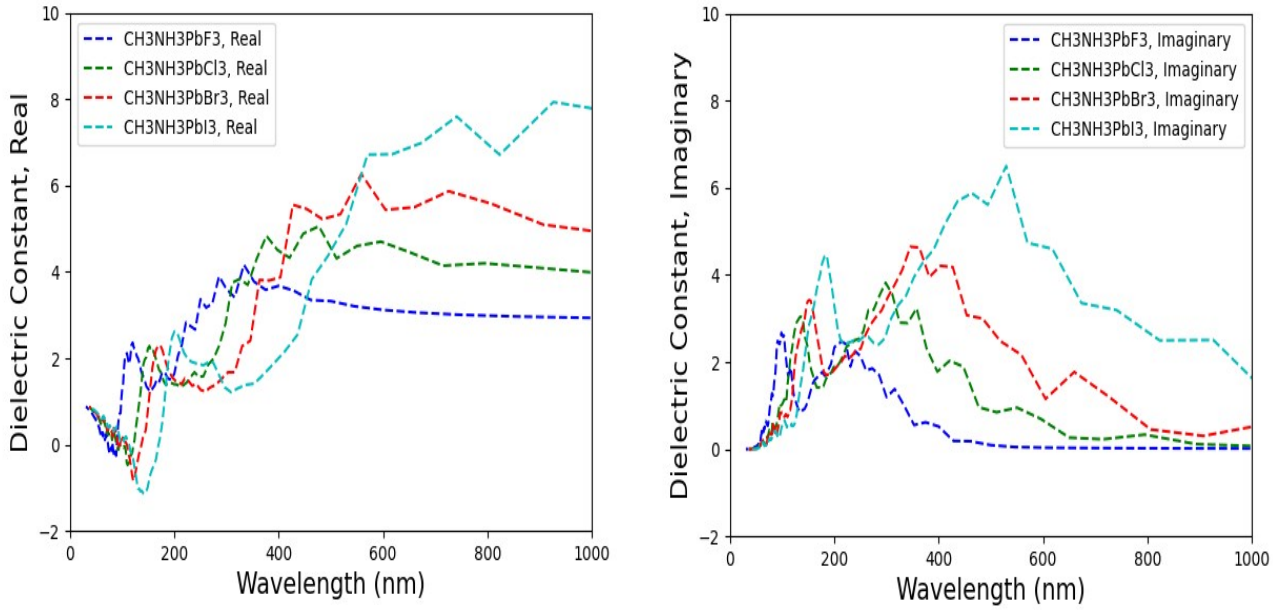

(a) (b)

Figure S10: Real (a) and imaginary (b) dielectric constants for (CH3NH3)PbX3 (X=F, Cl, Br, I) perovskites.

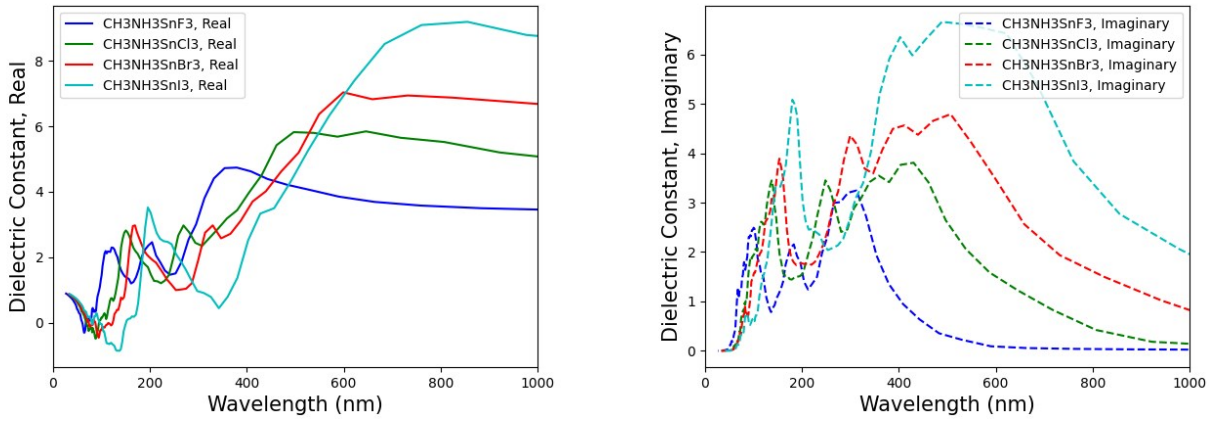

(a) (b)

Figure S11. The calculated dielectric matrix (without SOC) of (MA)SnX_3 perovskites by taking the average of diagonal elements (ε^{xx}, ε^{yy}, ε^{zz}). (a) Real part ε_1, (b) Imaginary part ε_2. Here, non-SOC calculations are presented for comparison with Figure 5 from the main document.

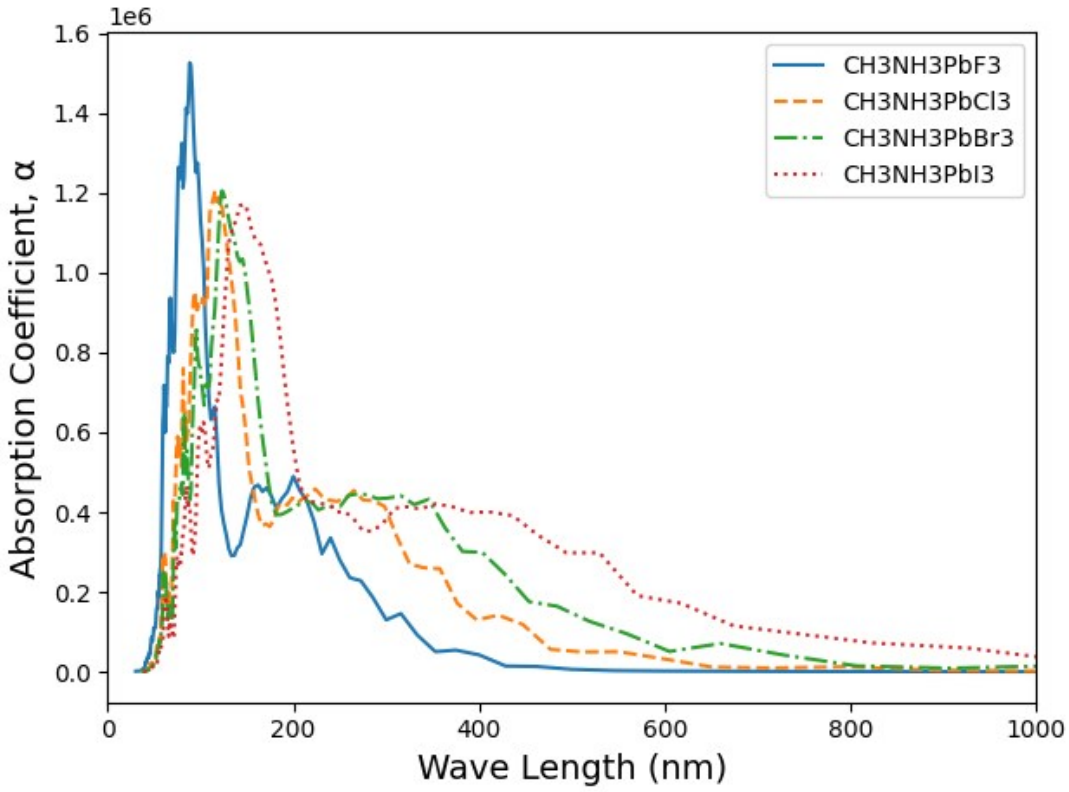

Figure S12: Absorption coefficients for $(CH_3NH_3)PbX_3$ (X=F, Cl, Br, I) perovskites.

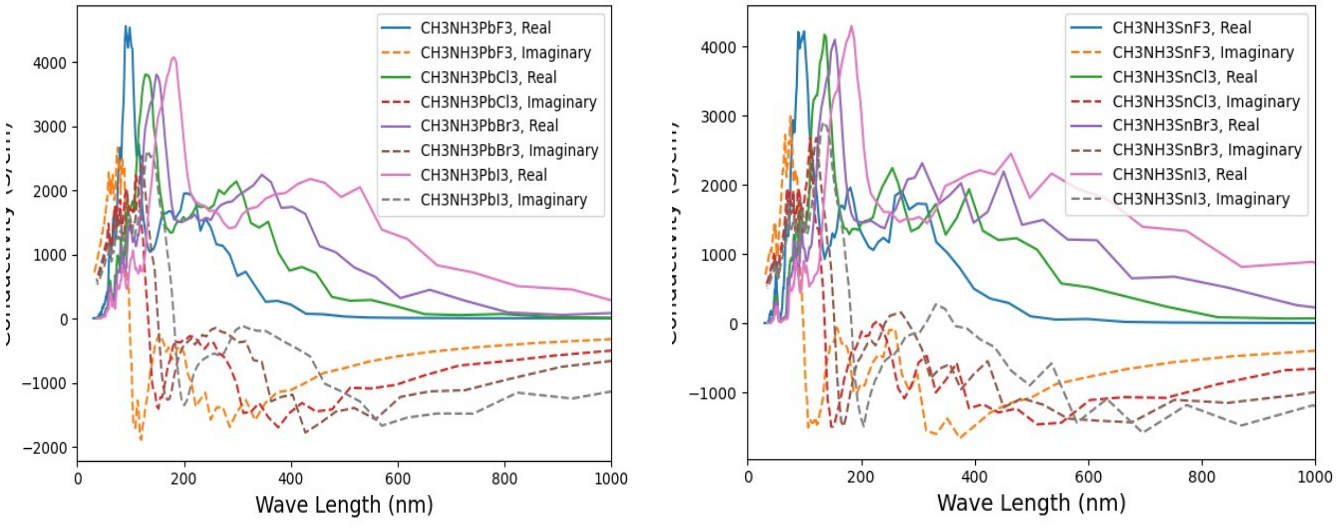

(a) (b)

Fig. S13 The calculated optical conductivities of (a) $(MA)PbX_3$; (b) $(MA)SnX_3$.

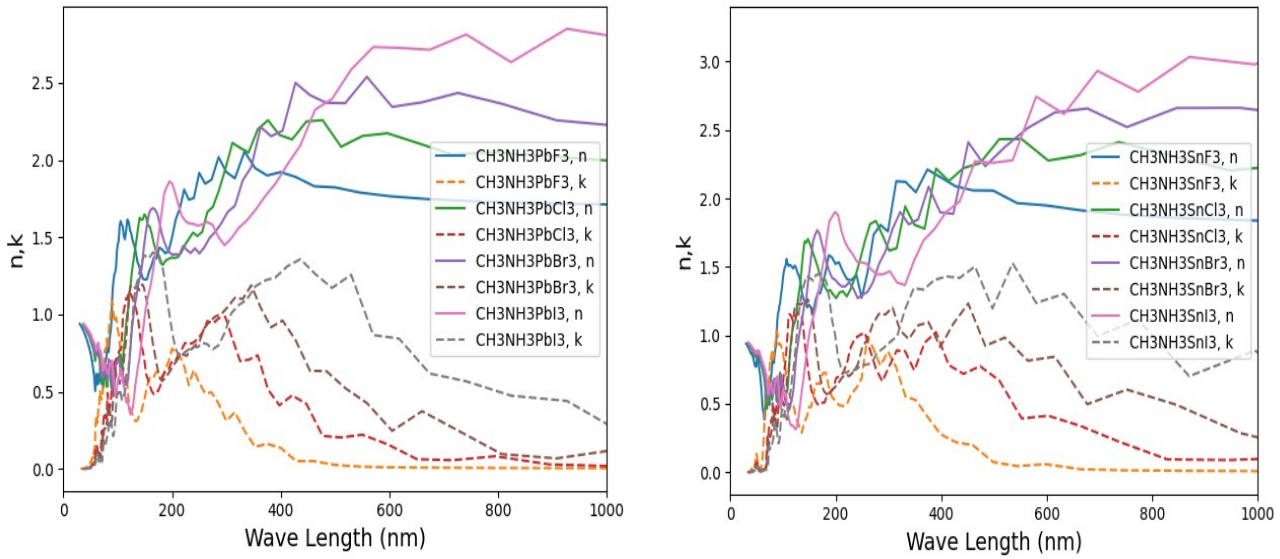

(a) (b)

Fig. S14 The calculated index of refraction (n) and the extinction coefficient (k) of (a) $(MA)PbX_3$; (b) $(MA)SnX_3$.

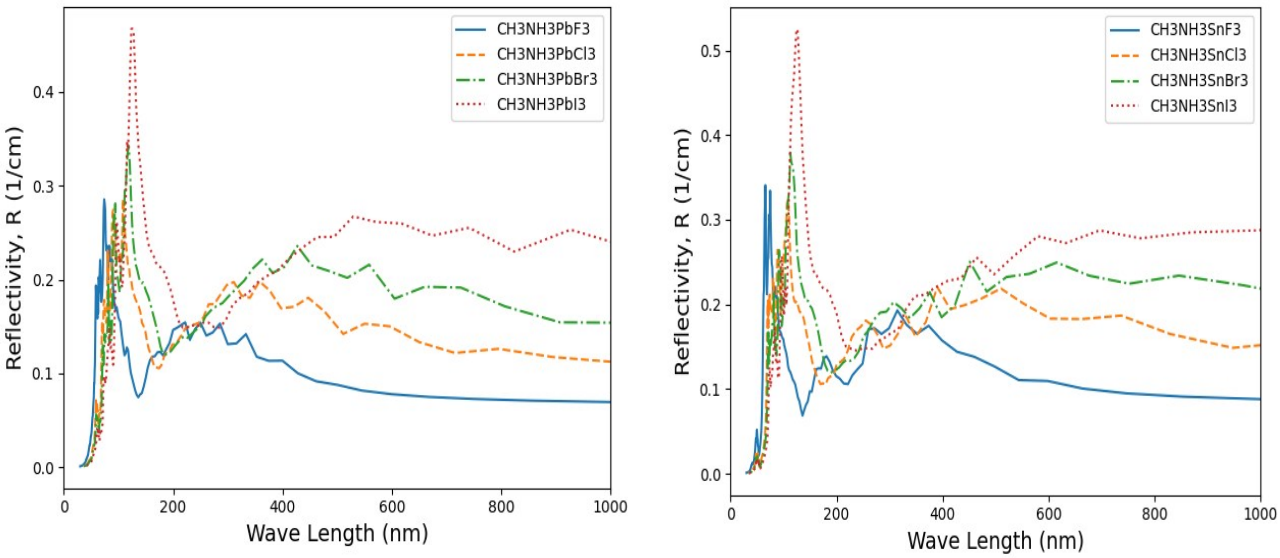

(a) (b)

Fig. S15 The calculated reflectivity (R) of (a) $(MA)PbX_3$; (b) $(MA)SnX_3$.

D.3 Metal Comparisons

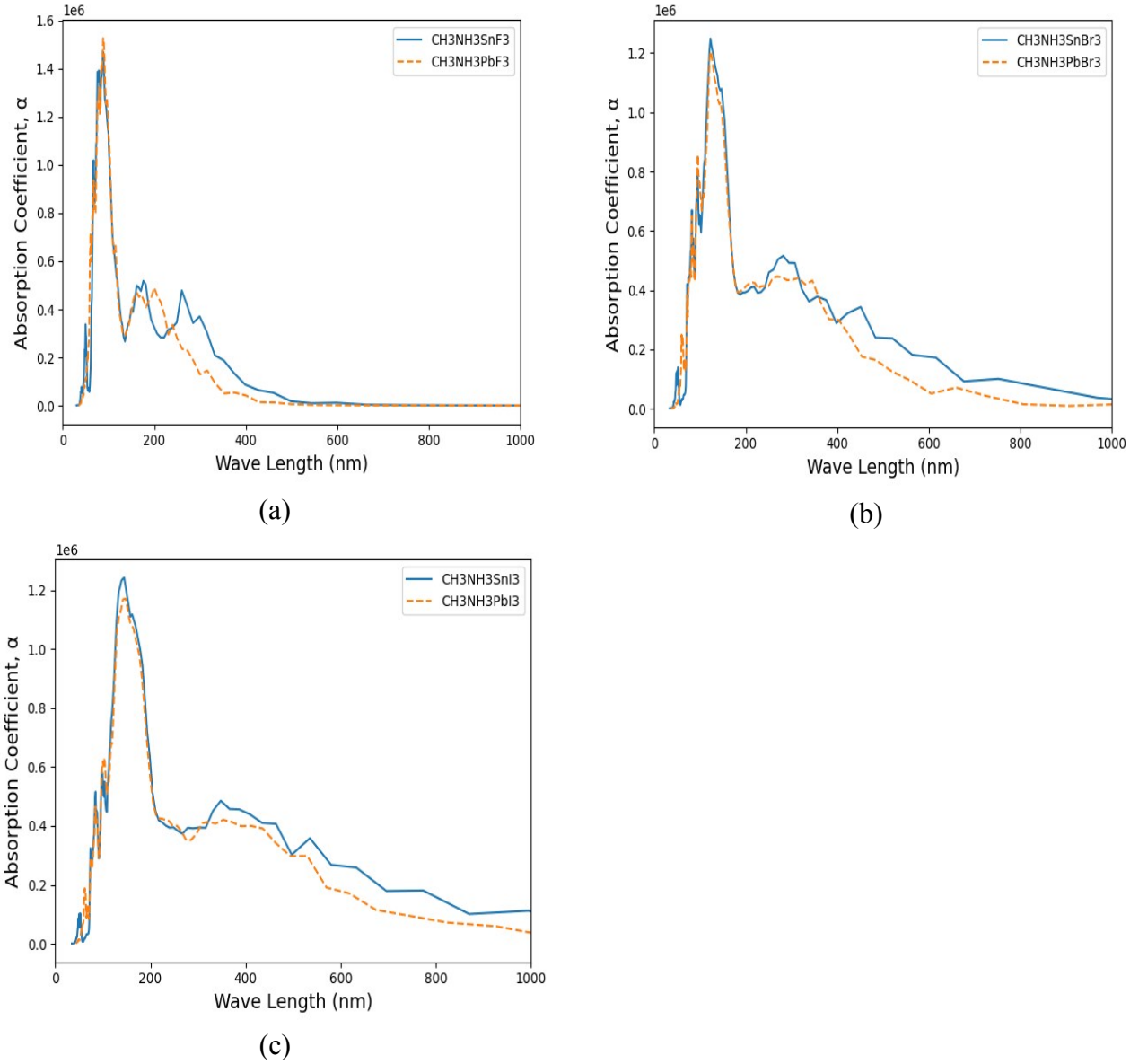

Fig. S16 Comparison of Absorption coefficients of (a) (MA)BF_3; (b) (MA)BBr_3; and (c) (MA)BI_3.

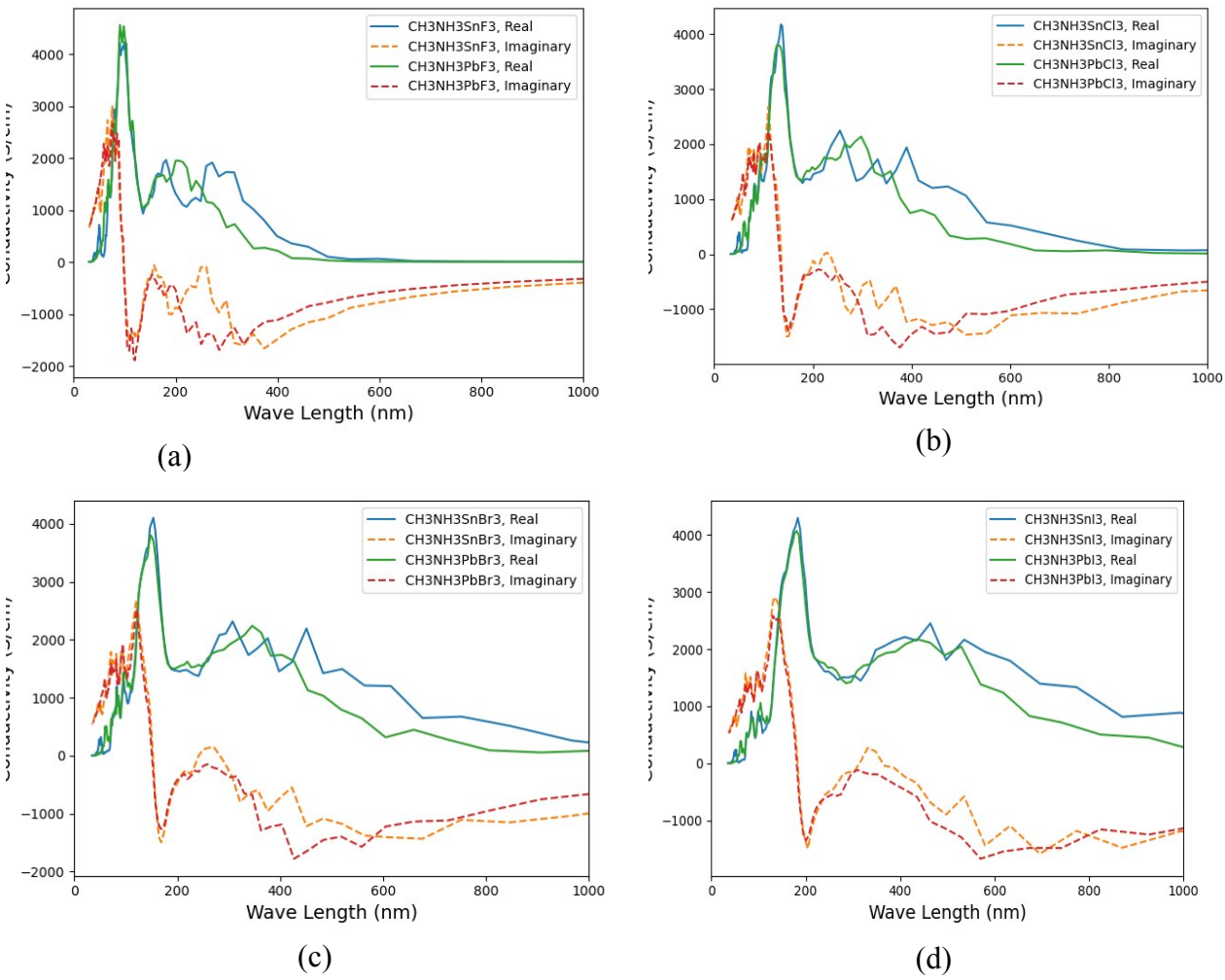

Fig.S17. Comparison of optical conductivity: (a) (MA)BF_3; (b) (MA)BCl_3; (c) (MA)BBr_3; (d) (MA)BI_3.

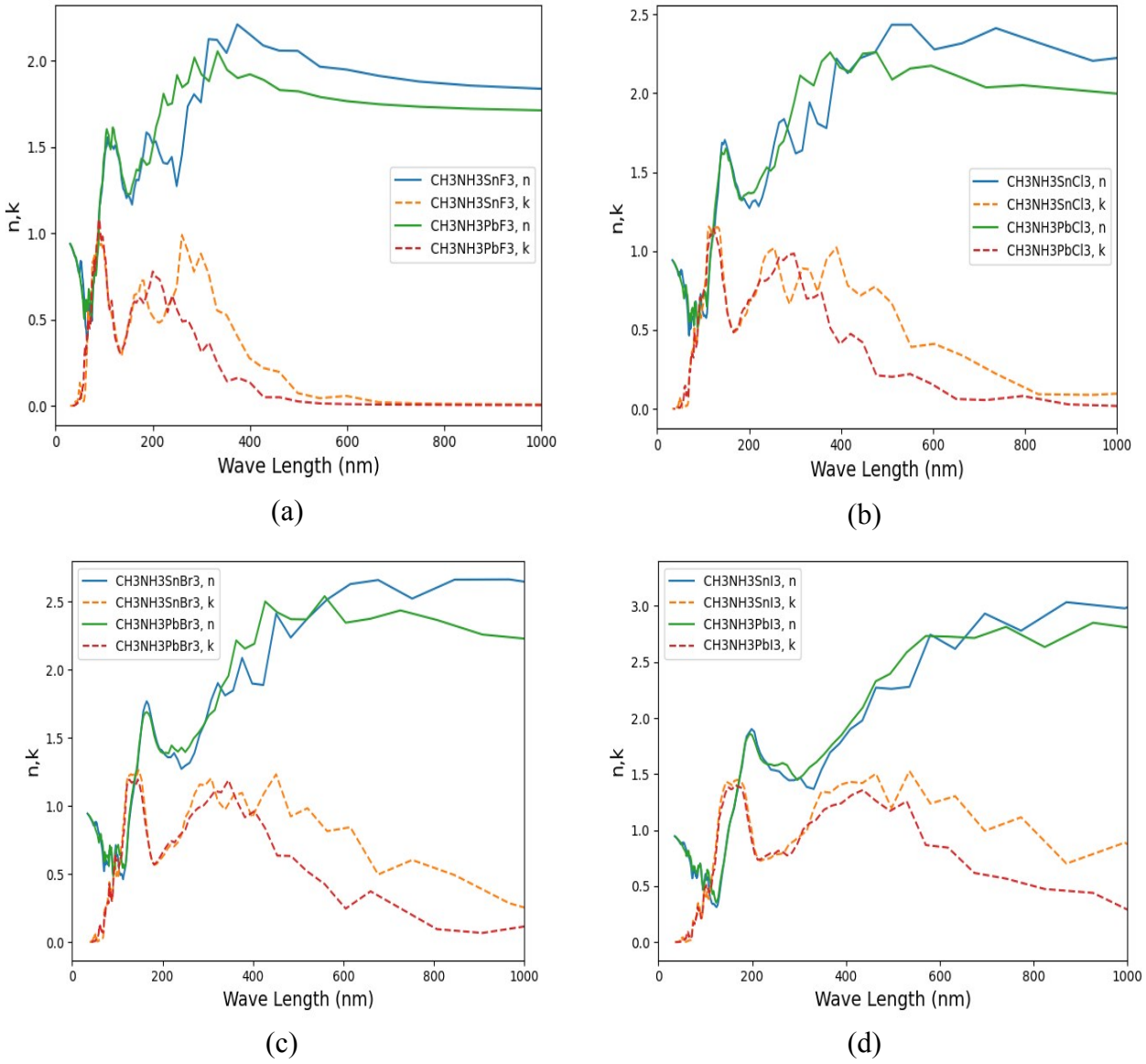

Fig.S18. Comparison of index of refraction (n) and the extinction coefficient (k): (a) (MA)BF_3; (b) (MA)BCl_3; (c) (MA)BBr_3; (d) (MA)BI_3.

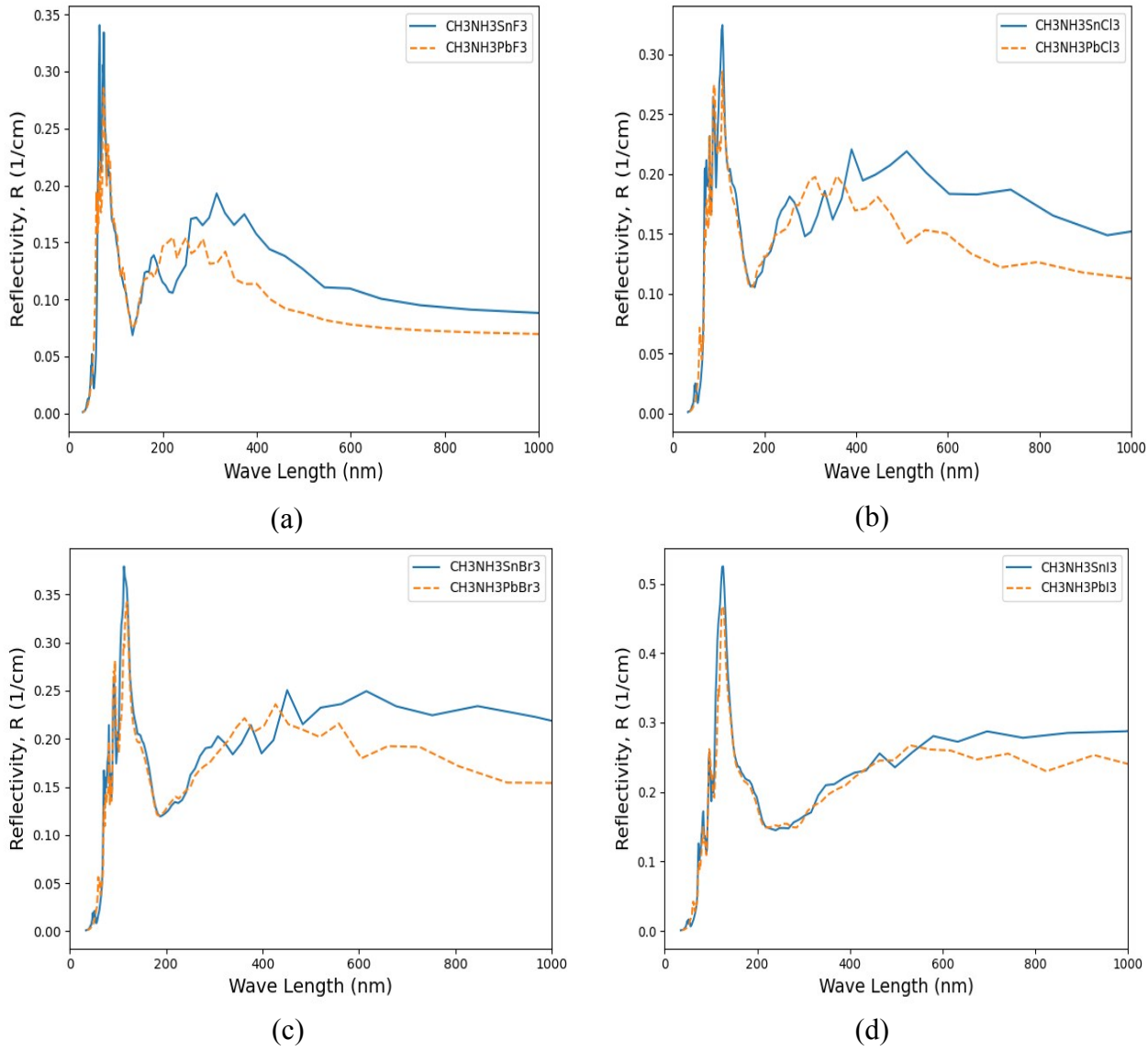

Fig.S19. Comparison of reflectivity (R): (a) $(MA)BF_3$; (b) $(MA)BCl_3$; (c) $(MA)BBr_3$; (d) $(MA)BI_3$.

Reference:

1. M. Gajdos, K. Hummer, G. Kresse, J. Furthmuller and F. Bechstedt, *Physical Review B*, 2006, **73**, 045112.
2. D. B. Tanner, in *Optical Effects in Solids*, Department of Physics, University of Florida, 2016.